Copyright ©2026
National Centre for Energy and Environment,
Energy Commission of Nigeria, University of Benin:
ISSN 2504-9593
DOI: 10.5281/zenodo.24626656
https://ijree.com/index.php/publications/article/view/104

Int. J. Renew. Energ & Environ Vol.4 (3), pp 46-58(2026)

EXPERIMENTAL INVESTIGATION OF A FRESNEL LENS SOLAR COOKER UNDER STAGNATION AND WATER-HEATING CONDITIONS FOR THERMODYNAMICS LABORATORY APPLICATIONS

***[1]Adamu, H., [2]Maina, M.B., [3]Muhammad, A.B.**

[1,2&3]Department of Mechanical Engineering, University of Maiduguri, Borno State Nigeria

*Corresponding author's e-mail address: hussainiadamu8813@gmail.com

Abstract

The thermal performance of a Fresnel lens solar cooker with an aperture area of 0.09 m² was evaluated experimentally. Two no-load (stagnation) tests were carried out on 31 August and 3 September 2026. Two load tests, with 1.0 kg and 1.5 kg of water, were carried out on 12 and 13 September 2026. Solar radiation, absorber plate temperature, cooker or water temperature, ambient temperature and wind speed were recorded at 15-minute intervals. The first figure of merit (F_1), second figure of merit (F_2) and cooking efficiency were calculated following the procedure of Mullick et al. (1987). The measured variables were then correlated with solar radiation by linear regression. Mean solar radiation over the four tests ranged from 816.68 to 896.81 W/m². The maximum absorber plate temperature was 114.0 °C at no load and 118.9 °C under load. The first figure of merit (F_1) was 0.0868 and 0.0638 °C·m²/W for the two no-load tests (mean 0.0753 °C·m²/W), which is below the benchmark of about 0.12 °C·m²/W quoted for box-type cookers, although that comparison is only indicative for a concentrating cooker. The second figure of merit (F_2) was 0.465 for the 1.0 kg load and 0.645 for the 1.5 kg load, both above the commonly quoted minimum of about 0.254. The cooking efficiency was 19.0 % and 33.2 % for the two loads respectively. Plate temperature correlated strongly with solar radiation on days of steady radiation (r = 0.83 to 0.88), whereas cloud interruptions and the heat drawn by the water weakened the correlation on the partly cloudy load-test day. The results show that the cooker heats water to near boiling temperature within about 4.75 to 5.25 hours under the prevailing conditions, and that steadiness of radiation matters more to performance than its instantaneous peak.

Keywords: Fresnel lens; solar cooker; stagnation test; figure of merit; cooking efficiency; solar radiation

1. Introduction

Solar cookers offer a clean alternative to firewood and fossil fuels for domestic cooking, especially in regions with high solar radiation. Concentrating cookers that use a Fresnel lens focus direct sunlight onto a small receiver plate and can reach much higher temperatures than box-type cookers, while the thin, light lens keeps the structure compact (Gorjian et al., 2022; Gorjian & Rahmati, 2024). The performance of solar cookers is usually reported using standardized indicators obtained from simple outdoor tests, following the procedure of Mullick et al. (1987), which was developed for box-type cookers. The first figure of merit (F_1), obtained from a no-load (stagnation) test, expresses the optical efficiency of the cooker relative to its heat loss factor (Mullick et al., 1987). The second figure of merit (F_2), obtained from a load test, describes how effectively the absorbed heat is transferred to the cooking load. The cooking efficiency is the fraction of the incident solar energy that is converted to useful heat in the water. Fresnel lens cookers have been studied analytically and in other climates, but there are few measured data that apply the standard figures of merit and the cooking efficiency to a locally fabricated Fresnel lens cooker under the semi-arid conditions of north-eastern Nigeria. This study addresses that gap. This paper reports the measured response of a Fresnel lens solar

cooker to solar radiation, ambient temperature and wind speed in two no-load tests and two load tests, and evaluates its thermal performance using F_1, F_2 and the cooking efficiency.

2. Materials and Methods

2.1 Materials

The cooker consisted of a Fresnel lens concentrator, a supporting frame with a tilt mechanism, and an insulated receiver box. The lens was a thin, flat plastic sheet with concentric grooves and an aperture area of 0.09 m². It was held in a dedicated lens holder fixed to a welded mild-steel frame that was coated with anti-corrosion paint and fitted with lockable castor wheels, a hinge and a threaded tilt arm for manual alignment of the lens with the sun.

The receiver box was a double-walled plywood box (plywood thickness 1.91 cm) with outer dimensions of 100 × 90 × 50 cm and inner dimensions of 88 × 78 × 35 cm. The 6 cm space between the walls was filled with sawdust insulation, and the inner box was painted black to increase absorption. The metal receiver (aluminium or mild steel) was coated with matte black paint and mounted at the focal point of the lens, and a glass cover was used as glazing to reduce heat loss. Water was used as the cooking load. The materials were sourced locally in Maiduguri.

Solar radiation was measured with a pyranometer, ambient temperature with a thermometer and wind speed with an anemometer, and the plate, cooker and water temperatures were measured with temperature sensors. Each variable was read at 15-minute intervals from about 10:00 AM to 4:00 PM, giving 25 readings per test (27 readings on 13 September, which started at 9:30 AM).

2.2 Methods

2.2.1 Test conditions

All tests were carried out outdoors in Maiduguri, Nigeria (11.85° N, 13.16° E, 325 m above sea level) under the prevailing weather conditions. No-load tests were performed on 31 August and 3 September 2026, and load tests with water as the cooking load on 12 September (1.0 L) and 13 September 2026 (1.5 L), between about 10:00 AM and 4:00 PM (9:30 AM start on 13 September). The density of water was taken as 1 kg/L, so 1.0 L and 1.5 L correspond to 1.0 kg and 1.5 kg.

2.2.2 Measurements and data treatment

Solar radiation, absorber plate temperature, cooker temperature (measured inside the cooker in the no-load tests and in the water in the cooking vessel in the load tests), ambient temperature and wind speed were recorded at 15-minute intervals. The average values quoted for each test are the arithmetic means of all recorded readings. In Figures 1 to 16, part (a) shows the variation of solar radiation and the measured variable with the time of day, and part (b) plots the variable against solar radiation with a linear best-fit line, its equation and the correlation coefficient (r).

2.2.3 Performance parameters

The first figure of merit is the difference between the absorber plate stagnation temperature and the ambient temperature, divided by the solar radiation at that time:

$$F_1 = \frac{(T_{ps} - T_{as})}{H_s} \quad (1)$$

where Tps is the maximum (stagnation) plate temperature (°C), Tas is the ambient temperature at that time (°C) and Hs is the solar radiation at that time (W/m²).

The second figure of merit, following Mullick et al. (1987), is:

$$F_2 = \frac{F_1 M C_w}{A\tau} \times \ln\left(\frac{\left[1 - \frac{(T_{w1} - T_a)}{F_1 H}\right]}{\left[1 - \frac{(T_{w2} - T_a)}{F_1 H}\right]}\right) \quad (2)$$

where M is the mass of water (kg), Cw is the specific heat capacity of water (4186 J/kg·K), A is the aperture area of the lens (0.09 m²), τ is the time taken for the water to heat from Tw1 to Tw2 (s), Ta is the average ambient temperature over that period (°C) and H is the average solar radiation over that period (W/m²). The heating range from about 40 °C to 90 °C was used for both load tests, because in this range the water heats steadily and is below boiling, which allows the two tests to be compared on the same basis.

The cooking efficiency is the ratio of the useful heat gained by the water to the solar energy incident on the lens aperture over the same period:

$$\eta = \frac{MC_w(T_{w2}-T_{w1})}{A\int G\,dt} \quad (3$$

where the integral of the solar radiation G over the heating period was evaluated from the 15-minute readings by the trapezoidal rule. The heating period was taken from the start of the test to the time of the maximum water temperature.

3. Results and Discussion

3.1 No-load tests

Solar radiation and absorber plate temperature. On 31 August, solar radiation increased from 869 W/m² at 10:00 AM to a peak of 955 W/m² at 11:00 AM, remained above 900 W/m² until approximately 12:15 PM, and then declined to 510 W/m² at 4:00 PM, averaging 816.68 W/m² (Figure 1). The plate temperature exceeded 100 °C between 10:45 AM and 12:45 PM, reaching a maximum of 114.0 °C at 12:45 PM, approximately 1 hour 45 minutes after peak radiation due to thermal energy accumulation. The mean plate temperature was 89.08 °C, with a strong positive correlation between radiation and temperature (r = 0.873).

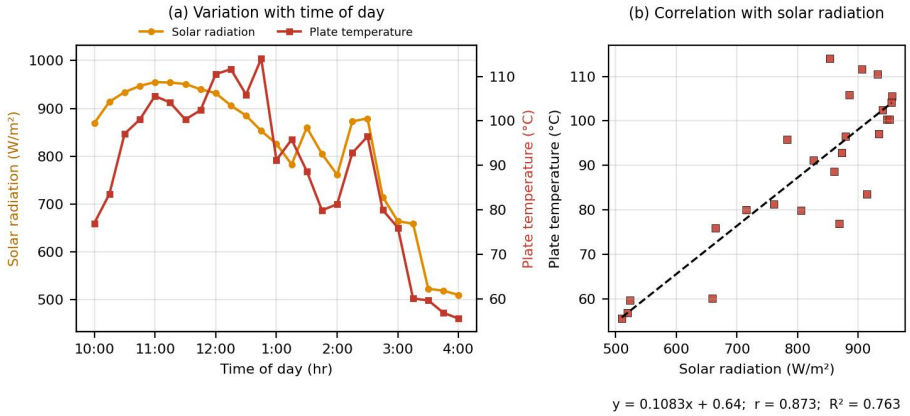

Figure 1: Solar radiation against absorber plate temperature (no-load test, 31 August 2026). (a) variation with time of day; (b) correlation with solar radiation.

On 3 September the radiation reached a maximum of 1016 W/m² at 12:30 PM and fell to 417 W/m² at 4:00 PM, with a mean of 833.72 W/m² (Figure 2). This is consistent with values reported for concentrating solar cookers: Gueymard (2021) gives about 1,000 W/m² for clear-sky beam irradiance at the surface and 700 to 1,000 W/m² for direct normal irradiance (DNI) at favourable sites. The mean is about 12.7 % higher than the 740 W/m² reported by Okonkwo et al. (2024) for a Fresnel lens cooker in Nigeria, and it is above the 700 to 780 W/m² of Thirugnanasambandam et al. (2023), the 700 W/m² design DNI of Jing et al. (2022) and the 600 W/m² minimum of the BIS/ASAE test standards, so the test conditions were valid. Two dips, to 699 W/m² at 11:15 AM and 752 W/m² at 2:30 PM, are typical of passing cloud (Nkwetta et al., 2023). The plate responded to the first dip immediately, falling by 19.7 °C in one 15-minute step

(89.5 °C to 69.8 °C) and recovering to 93.6 °C by 11:45 AM. This suggests that the plate stores relatively little thermal energy and responds quickly to changes in solar input, but increased convective or radiative heat losses may also contribute, so a low thermal mass is a plausible explanation rather than a definitive conclusion. The maximum plate temperature was 103.7 °C at 1:00 PM, the mean was 83.74 °C, and the correlation with radiation was strong (r = 0.884, slope about 0.081 °C per W/m²).

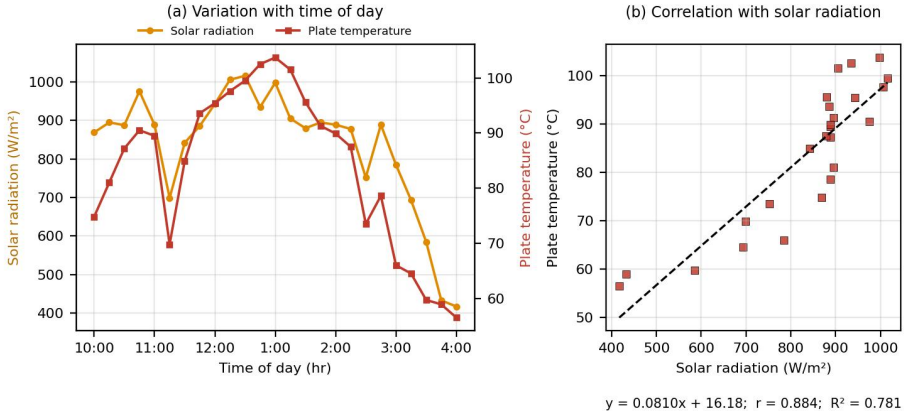

Figure 2: Solar radiation against absorber plate temperature (no-load test, 3 September 2026). (a) variation with time of day; (b) correlation with solar radiation.

Cooker temperature. On 31 August (Figure 3), the cooker temperature increased from 40.5 °C to 84.5 °C by 11:00 AM and peaked at 98.5 °C at 12:15 PM. It lagged the plate by up to 36.5 °C in the morning but remained 4–5 °C hotter during late-afternoon cooling, indicating better heat retention. The mean temperature was 78.96 °C (r = 0.517). On 3 September (Figure 4), the temperature rose from 46.5 °C to a maximum of 91.5 °C at 1:00 PM, averaging 74.24 °C (r = 0.639). During the cloud-induced dip at 11:15 AM, the cooker temperature fell by only about 2 °C, compared with 19.7 °C for the plate, which shows its greater thermal inertia and reduced sensitivity to short-term fluctuations.

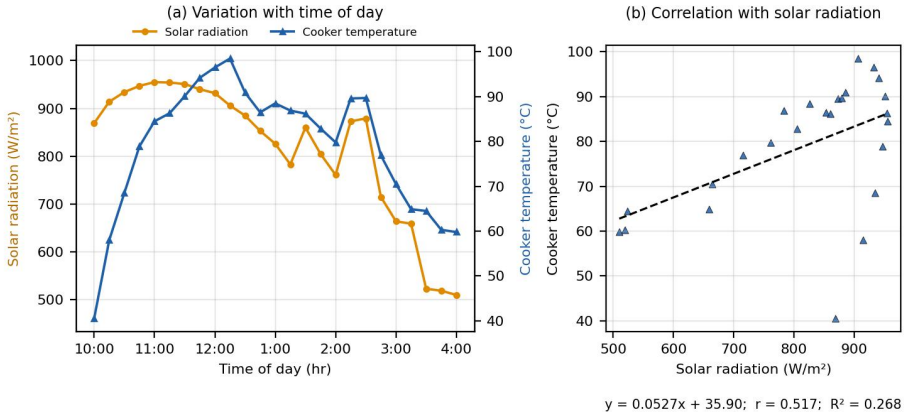

Figure 3: Solar radiation against cooker temperature (no-load test, 31 August 2026). (a) variation with time of day; (b) correlation with solar radiation.

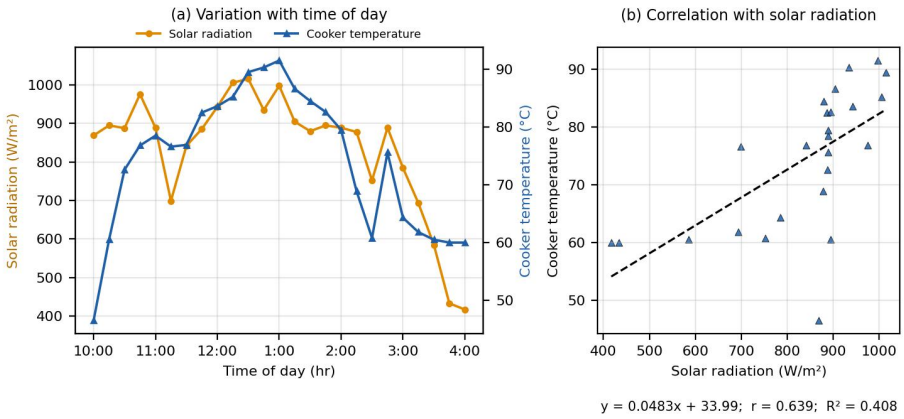

Figure 4: Solar radiation against cooker temperature (no-load test, 3 September 2026). (a) variation with time of day; (b) correlation with solar radiation.

Ambient temperature and wind speed. The ambient temperature ranged from 30.1 to 41.9 °C (mean 38.39 °C) on 31 August and from 34.8 to 41.4 °C (mean 38.09 °C) on 3 September (Figures 5 and 7). In both tests it peaked well after the radiation peak (by about 2 hours 45 minutes and 3 hours 15 minutes respectively), reflecting the thermal lag of the ground and surrounding air, which explains the negative correlations with radiation (r = −0.417 and −0.358). Wind speed was low on both days (Figures 6 and 8), with means of 0.672 m/s (maximum 2.4 m/s) and 0.276 m/s (maximum 1.4 m/s). The plate temperature continued to rise during the strongest gusts, and on 3 September the maximum plate and cooker temperatures occurred at a wind speed of only 0.3 m/s, so the difference between the two no-load days cannot be attributed mainly to wind.

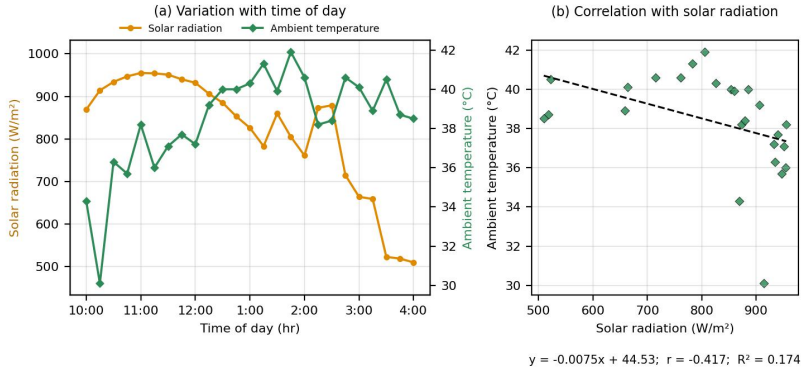

Figure 5: Solar radiation against ambient temperature (no-load test, 31 August 2026). (a) variation with time of day; (b) correlation with solar radiation.

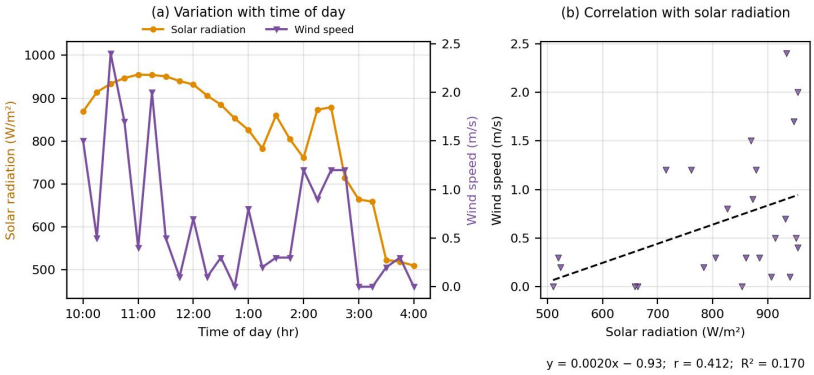

Figure 6: Solar radiation against wind speed (no-load test, 31 August 2026). (a) variation with time of day; (b) correlation with solar radiation.

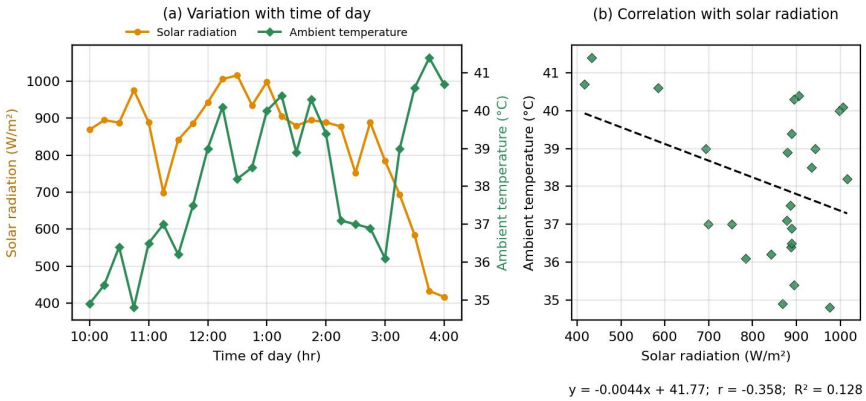

Figure 7: Solar radiation against ambient temperature (no-load test, 3 September 2026). (a) variation with time of day; (b) correlation with solar radiation.

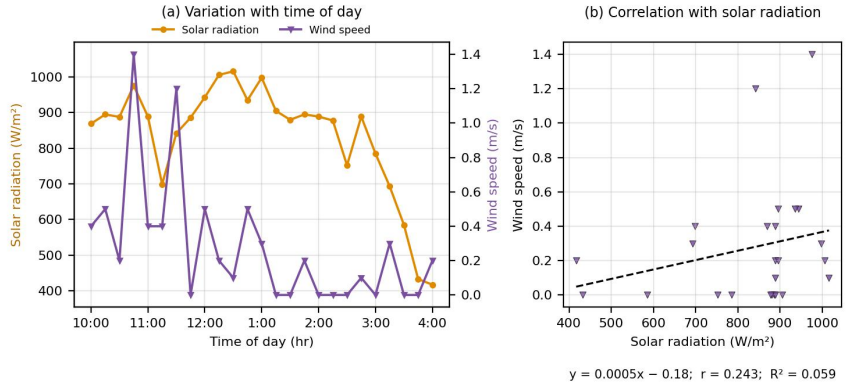

Figure 8: Solar radiation against wind speed (no-load test, 3 September 2026). (a) variation with time of day; (b) correlation with solar radiation.

Comparison of the two no-load tests (Figures 1 to 8) shows that, although the mean radiation on 3 September was about 2 % higher than on 31 August, the mean plate temperature was 5.3 °C lower and the mean cooker temperature 4.7 °C lower. On 31 August the radiation was high and uninterrupted (869 to 955 W/m² from 10:00 AM to 12:15 PM), which allowed the cooker to heat continuously, whereas on 3 September it was interrupted by cloud. The cooker performance therefore depends more on the steadiness of the radiation than on its instantaneous peak value.

3.2 Load tests

12 September (1.0 kg of water). The day was partly cloudy: radiation rose from 735 W/m² to a maximum of 1027 W/m² at 12:15 PM, with dips to 867, 788 and 645 W/m², and fell to 598 W/m² by 4:00 PM (mean 857.88 W/m²). The plate (Figure 9) started at 30.5 °C, below the ambient temperature, reached a maximum of 99.7 °C at 1:30 PM and then stayed almost constant at 95.6 to 96.2 °C from 2:00 to 3:00 PM although radiation varied between 645 and 896 W/m², which shows that the plate was passing heat to the water at about the rate at which it received it. The mean plate temperature was 73.78 °C, lower than in the no-load tests because of the cold start and the heat drawn away by the water. The correlation with radiation was almost zero ($r = -0.025$). This does not mean that radiation has no effect: in a load test the plate temperature is governed by the accumulated energy and by the heat drawn away by the water, so the warm-up and afternoon branches cancel out in a straight-line fit.

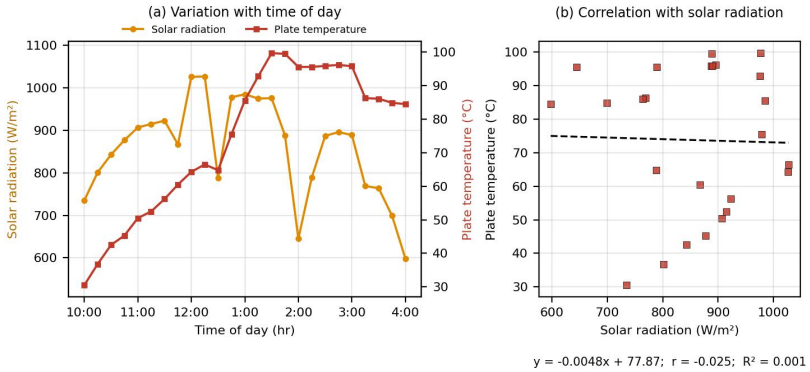

Figure 9: Solar radiation against absorber plate temperature (load test, 12 September 2026, 1.0 kg water). (a) variation with time of day; (b) correlation with solar radiation.

The water (Figure 10) was heated from 31.3 °C at 10:00 AM to a maximum of 93.5 °C at 2:45 PM without reaching boiling, at an average rate of about 16.7 °C per hour between 10:00 AM and 1:30 PM. After 1:15 PM it stayed between 86.9 and 93.5 °C and fell only to 87.6 °C at 4:00 PM, even though radiation had dropped to 598 W/m². At 3:15 PM the water (91.1 °C) was hotter than the plate (86.3 °C), which shows the thermal storage effect of the water. The mean water temperature was 70.48 °C, and its correlation with radiation was very weak (r = −0.129) because the water temperature is a cumulative response that lags the radiation by more than an hour. The ambient temperature (Figure 11) ranged from 33.7 to 38.7 °C (mean 36.56 °C, the lowest of the four days) and the wind was very low (Figure 12; mean 0.26 m/s, with a single gust of 2.5 m/s during which the plate and water temperatures kept rising), so wind was not a limiting factor.

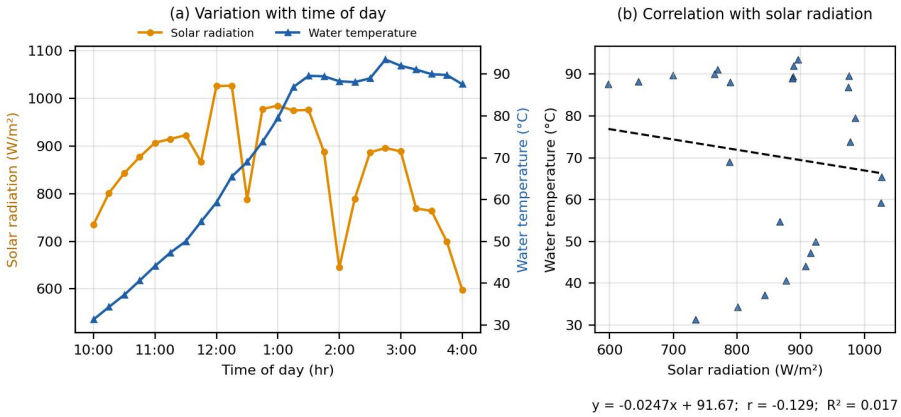

Figure 10: Solar radiation against water temperature (load test, 12 September 2026, 1.0 kg water). (a) variation with time of day; (b) correlation with solar radiation.

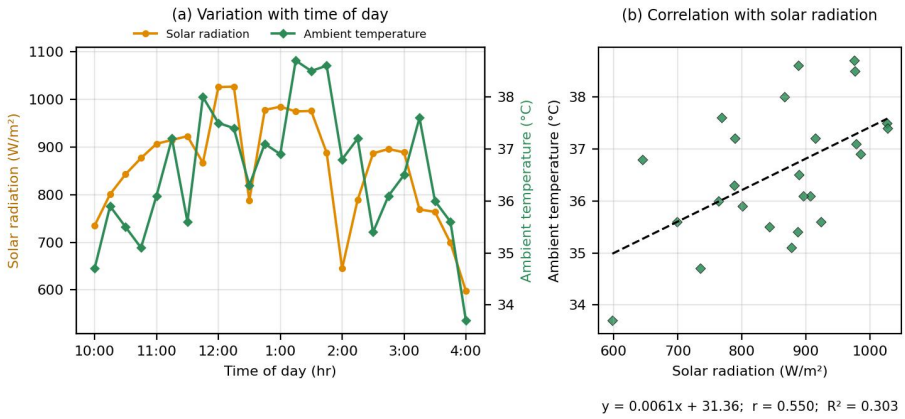

Figure 11: Solar radiation against ambient temperature (load test, 12 September 2026). (a) variation with time of day; (b) correlation with solar radiation.

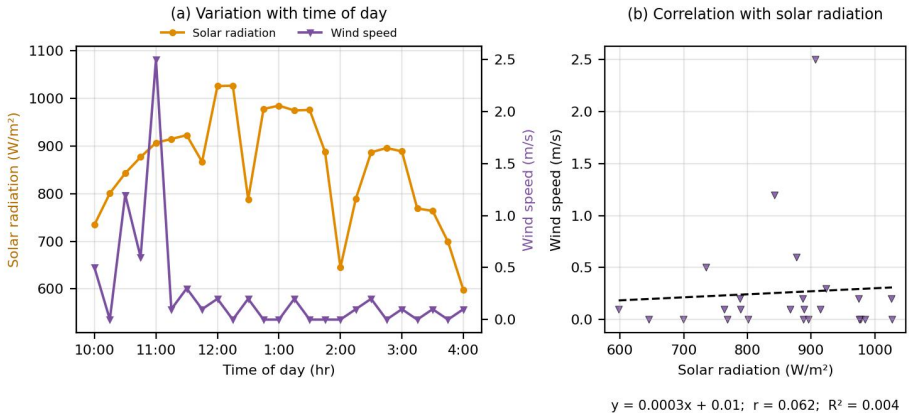

Figure 12: Solar radiation against wind speed (load test, 12 September 2026). (a) variation with time of day; (b) correlation with solar radiation.

13 September (1.5 kg of water). This was the clearest day of the four: radiation rose from 689 W/m² at 9:30 AM to 904 W/m² by 11:00 AM and then stayed between 886 and 999 W/m² until 3:00 PM, with the highest mean of the four tests (896.81 W/m²). The plate temperature (Figure 13) rose to 100.5 °C at 12:45 PM, stayed at about 98 to 101 °C between 1:15 and 2:00 PM and then rose to a maximum of 118.9 °C at 2:45 PM (radiation 999 W/m², ambient 43.5 °C), the highest plate temperature of all the tests. The mean was 83.81 °C. The correlation with radiation was strong (r = 0.833) and the slope of about 0.235 °C per W/m² was the steepest of the four days, because the plate accumulates heat continuously under sustained high radiation. Since the plate temperature under load exceeded the maximum recorded in both no-load tests (114.0 and 103.7 °C), the no-load tests probably did not achieve true stagnation conditions.

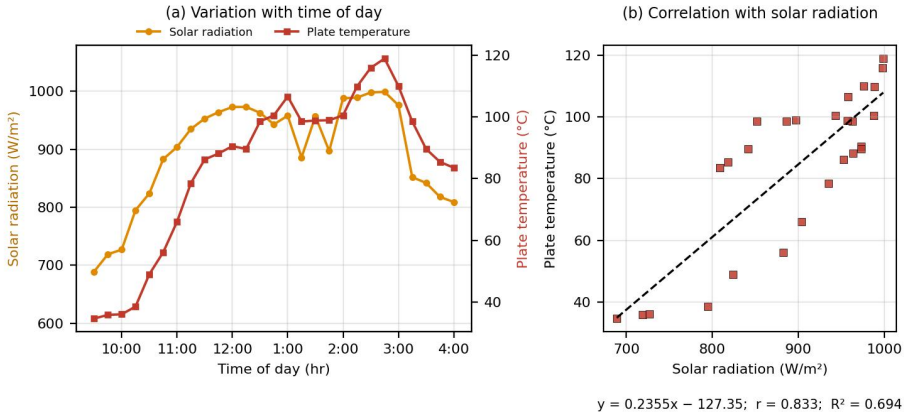

Figure 13: Solar radiation against absorber plate temperature (load test, 13 September 2026, 1.5 kg water). (a) variation with time of day; (b) correlation with solar radiation.

The water (Figure 14) was heated from 30.5 °C and gained only 14.7 °C in the first 1.5 hours because the larger mass needs more energy and the plate was still warming up. It then heated at about 20.9 °C per hour from 11:00 AM to 1:00 PM (45.2 to 86.9 °C) and reached 99.5 °C at 2:00 PM. The recorded maximum of 112.3 °C at 2:45 PM, and the readings of 101.8, 110.5, 112.3 and 109.4 °C between 2:15 and 3:00 PM, exceed the boiling point of water at atmospheric pressure. Water in an open vessel cannot exceed about 100 °C, so either the vessel was covered or sealed so that steam pressure built up, or the probe was influenced by vapour or by the hot vessel wall; these values should be interpreted with care. The mean water temperature was 71.13 °C and the correlation with radiation was moderate (r = 0.599). The larger water mass reached a higher temperature than on 12 September because the radiation was more intense and steadier and the ambient temperature was higher (Figure 15; mean 39.07 °C, rising to 43.5 °C at 2:45 PM), which reduced the temperature difference between the plate and the surroundings and therefore the heat loss. Wind speed was low (Figure 16; mean 0.311 m/s) and had no noticeable effect on the heating process.

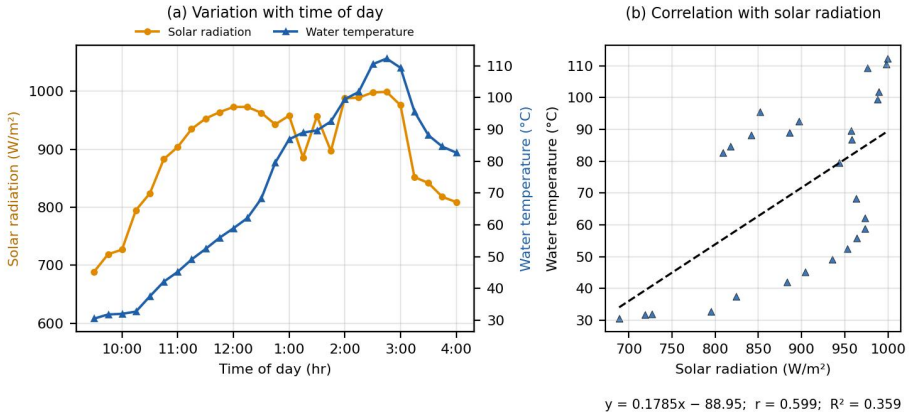

Figure 14: Solar radiation against water temperature (load test, 13 September 2026, 1.5 kg water). (a) variation with time of day; (b) correlation with solar radiation.

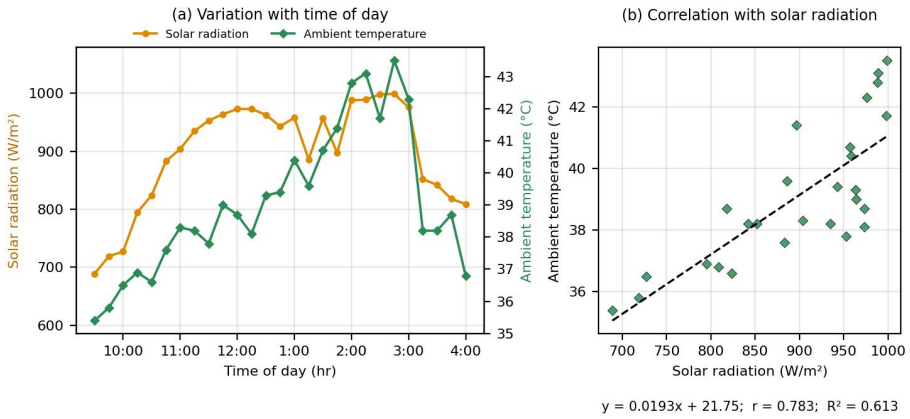

Figure 15: Solar radiation against ambient temperature (load test, 13 September 2026). (a) variation with time of day; (b) correlation with solar radiation.

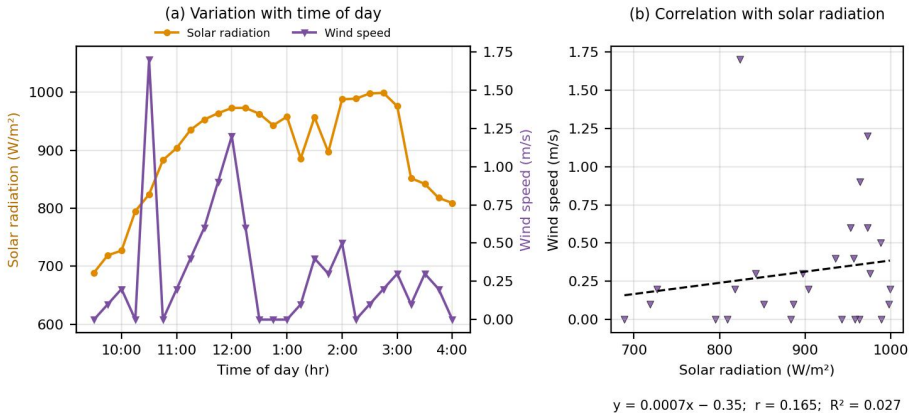

Figure 16: Solar radiation against wind speed (load test, 13 September 2026). (a) variation with time of day; (b) correlation with solar radiation.

Across the two load tests (Figures 9 to 16), the cooker heated 1.0 kg of water to 93.5 °C and 1.5 kg of water to above 100 °C (subject to the caution on the vessel above) in about 4.75 and 5.25 hours from the start of the test respectively.

3.3 Correlation of the measured variables with solar radiation

The correlation coefficients (r) between solar radiation and each measured variable are given in part (b) of Figures 1 to 16. The plate temperature had the strongest relationship with radiation in three of the four tests (r = 0.83 to 0.88), because it receives the concentrated energy directly. The cooker or water temperature was less strongly correlated (r = 0.52 to 0.64 where the response was clear) because it responds with a delay. The ambient temperature showed weak to moderate correlation (r = −0.42 to 0.78), with a sign that depends on the timing of its peak relative to the radiation peak, and wind speed showed no consistent relationship (r = 0.06 to 0.41). The very low correlations for the 12 September plate and water temperatures (r = −0.025 and −0.129) result from the cloud interruptions and the transient nature of the load test, not from an absence of dependence on radiation.

3.4 Thermal performance

First figure of merit. F_1 was 0.0868 °C·m²/W for 31 August, from (114.0 − 40.0)/853, and 0.0638 °C·m²/W for 3 September, from (103.7 − 40.0)/998. The mean of 0.0753 °C·m²/W is lower than the value of about 0.12 °C·m²/W commonly quoted as the acceptable minimum for box-type solar cookers; since that standard

was written for box cookers, the comparison for a concentrating Fresnel lens cooker is indicative only. Two reasons are likely. First, the receiver plate of a lens cooker is exposed and hot at a small focal spot, so its heat loss to the surroundings is high compared with a well-insulated box cooker. Second, the stagnation temperature was probably not fully reached in the no-load tests, because the radiation was interrupted by cloud and any small tracking error moves the focal spot off the plate. In support of this, the plate reached 118.9 °C under load on 13 September at 2:45 PM, which gives (118.9 − 43.5)/999 = 0.0755 °C·m²/W, so the F_1 values presented here should be regarded as conservative.

Second figure of merit. F_2 was 0.465 for the 1.0 kg test and 0.645 for the 1.5 kg test. Both values are above the value of about 0.254 commonly quoted as the minimum acceptable F_2 for box-type cookers, and show that heat is transferred efficiently from the absorber plate to the water. The higher F_2 on 13 September reflects the steadier radiation on that day and the better heat transfer to the larger water mass. Because F_2 is calculated from F_1, it is sensitive to the F_1 value chosen: using the individual values of 0.0868 and 0.0638 instead of the mean gives F_2 between 0.41 and 0.61 for 12 September and between 0.57 and 0.82 for 13 September. In all cases the cooker meets the minimum benchmark.

Cooking efficiency. The cooking efficiency (η) was 19.0 % for the 1.0 kg load and 33.2 % for the 1.5 kg load. It is higher for the larger mass for three reasons. A larger water mass absorbs a greater share of the energy available at the plate, and the heat losses, which depend mainly on plate and ambient temperature rather than on the water mass, form a smaller fraction of the total. The radiation on 13 September was also more intense and steady, whereas the 12 September test was affected by intermittent cloud and the plate and water temperatures levelled off between 2:00 and 4:00 PM while radiation was low. Since the two tests were done on different days with different loads, the effects of load and weather cannot be separated exactly. The efficiency over the 40 to 90 °C heating range (24.5 % and 35.6 %) follows the same trend and is higher than the full-period value in both tests because the early warm-up, when much of the energy heats the cold plate and cooker rather than the water, is excluded. For the 13 September test, stopping the calculation when the water first reaches 99.5 °C (2:00 PM) still gives 33.2 %, so the result does not depend on the readings above 100 °C.

4. Conclusions

This study set out to measure the response of a Fresnel lens solar cooker (aperture area 0.09 m²) to solar radiation, ambient temperature and wind speed, and to evaluate its thermal performance using the first and second figures of merit and the cooking efficiency. Both objectives were achieved. The absorber plate reached 114.0 °C at no load and 118.9 °C under load and was strongly correlated with solar radiation on days of steady radiation (r = 0.83 to 0.88), whereas the cooker interior and the water responded with a delay and damped short-lived changes in radiation. The rapid plate response is consistent with a low thermal mass, although increased heat loss may also contribute. Performance depended more on the steadiness of the radiation than on its instantaneous peak value, and wind speed (0.0 to 2.5 m/s) had no noticeable effect on the heating process in any test.

The cooker heated 1.0 kg of water to 93.5 °C and 1.5 kg of water to above 100 °C in about 4.75 to 5.25 hours. The mean first figure of merit was 0.0753 °C·m²/W, below the

0.12 °C·m²/W benchmark for box-type cookers, although this benchmark is only indicative for a concentrating cooker and the value is probably conservative because stagnation was not fully reached. The second figure of merit was 0.465 for 1.0 kg and 0.645 for 1.5 kg of water, both above the commonly quoted minimum of 0.254, and the cooking efficiency was 19.0 % and 33.2 % respectively (24.5 % and 35.6 % over the 40 to 90 °C range). Because the loads were tested on different days, the effects of load and weather cannot be separated exactly, and the water readings above 100 °C on 13 September should be treated with care. Repeated runs under the same load and weather conditions, with the vessel arrangement and probe position recorded, are recommended.

References

Gorjian, A., & Rahmati, E. (2024). A thermodynamic review on concentrating type solar cookers. Solar Energy. https://doi.org/10.1016/j.solener.2024.008545

Gorjian, A., Rahmati, E., Gorjian, S., Anand, A., & Jathar, L. D. (2022). A comprehensive study of research and development in concentrating solar cookers (CSCs): design considerations, recent advancements, and economics. Solar Energy, 245, 80–107. https://doi.org/10.1016/j.solener.2022.08.066

Goyal, R. K., & Eswaramoorthy, M. (2024). Theoretical and experimental analysis of box-type solar cooker with sensible heat storage. Solar Energy, 268, 112273. https://doi.org/10.1016/j.solener.2024.112273

Gueymard, C. A. (2021). A reevaluation of the solar constant based on a 42-year total solar irradiance record and new spectral measurements: Implications for solar resource assessment. *Solar Energy,* 228, 17–36. https://doi.org/10.1016/j.solener.2021.09.050

Gupta, M., Singh, P. L., & Pande, G. S. (2022). Finite element analysis of temperature distribution in cooking pot materials under concentrated solar flux from a Fresnel lens. *Applied Thermal Engineering,* 210, 118345. https://doi.org/10.1016/j.applthermaleng.2022.118345

Hassan, Q., Abbas, M. K., Tabar, M. Y., & Salman, H. M. (2023). Impact of Saharan aerosol events on the optical and thermal performance of Fresnel lens solar cookers in North Africa. *Renewable Energy,* 212, 877–891. https://doi.org/10.1016/j.renene.2023.05.078

Incropera, F. P., DeWitt, D. P., Bergman, T. L., & Lavine, A. S. (2013). Principles of Heat and Mass Transfer (7th ed.). John Wiley & Sons.

International Energy Agency. (2023). World energy outlook 2023: Energy access and clean cooking. *IEA Publications.* https://www.iea.org/reports/world-energy-outlook-2023

Jing, L., Liu, Z., & Ding, W. (2022). Open-source groove profile optimisation for Fresnel lens solar concentrators and application to silicone-on-glass designs. *Solar Energy,* 242, 168–181. https://doi.org/10.1016/j.solener.2022.07.018

Mullick, S. C., Kandpal, T. C., & Saxena, A. K. (1987). Thermal test procedure for box-type solar cookers. Solar Energy, 39(4), 353–360. https://doi.org/10.1016/S0038-092X(87)80021-5

Newport Corporation. (2022). Introduction to Solar Radiation. https://www.newport.com/t/introduction-to-solar-radiation/

Nkwetta, D. N., Smyth, M., & Zacharopoulos, A. (2023). Dynamic tilt-angle optimisation and cloud-transient thermal mass sizing for concentrating solar cookers deployed in tropical Africa. *Applied Thermal Engineering,*

230, 120625. https://doi.org/10.1016/j.applthermaleng.2023.120625

Okonkwo, E. C., Wole-Osho, I., Almanassra, I. W., & Mahian, O. (2024). Exergy analysis and irreversibility mapping of a circular Fresnel lens solar cooker operating in Nigeria. *Renewable Energy,* 222, 119789. https://doi.org/10.1016/j.renene.2024.119789

Thirugnanasambandam, M., Iniyan, S., & Goic, R. (2023). Performance evaluation of a Fresnel lens concentrating solar cooker integrated with an evacuated tube absorber. *Solar Energy,* 259, 89–103. https://doi.org/10.1016/j.solener.2023.05.012